

## ORIGINAL ARTICLE

## CD99 suppresses osteosarcoma cell migration through inhibition of ROCK2 activity

C Zucchini<sup>1</sup>, MC Manara<sup>2,3</sup>, RS Pinca<sup>2,3</sup>, P De Sanctis<sup>1</sup>, C Guerzoni<sup>3,4</sup>, M Sciandra<sup>2</sup>, P-L Lollini<sup>1</sup>, G Cenacchi<sup>5</sup>, P Picci<sup>3</sup>, L Valvassori<sup>1</sup> and K Scotlandi<sup>2,3,4</sup>

CD99, a transmembrane protein encoded by *MIC2* gene is involved in multiple cellular events including cell adhesion and migration, apoptosis, cell differentiation and regulation of protein trafficking either in physiological or pathological conditions. In osteosarcoma, CD99 is expressed at low levels and functions as a tumour suppressor. The full-length protein (CD99wt) and the short-form harbouring a deletion in the intracytoplasmic domain (CD99sh) have been associated with distinct functional outcomes with respect to tumour malignancy. In this study, we especially evaluated modulation of cell–cell contacts, reorganisation of the actin cytoskeleton and modulation of signalling pathways by comparing osteosarcoma cells characterised by different metastasis capabilities and CD99 expression, to identify molecular mechanisms responsible for metastasis. Our data indicate that forced expression of CD99wt induces recruitment of N-cadherin and  $\beta$ -catenin to adherens junctions. In addition, transfection of CD99wt inhibits the expression of several molecules crucial to the remodelling of the actin cytoskeleton, such as ACTR2, ARPC1A, Rho-associated, coiled-coil containing protein kinase 2 (ROCK2) as well as ezrin, an ezrin/radixin/moesin family member that has been clearly associated with tumour progression and metastatic spread in osteosarcoma. Functional studies point to ROCK2 as a crucial intracellular mediator regulating osteosarcoma migration. By maintaining c-Src in an inactive conformation, CD99wt inhibits ROCK2 signalling and this leads to ezrin decrease at cell membrane while N-cadherin and  $\beta$ -catenin translocate to the plasma membrane and function as main molecular bridges for actin cytoskeleton. Taken together, we propose that the re-expression of CD99wt, which is generally present in osteoblasts but lost in osteosarcoma, through inhibition of c-Src and ROCK2 activity, manages to increase contact strength and reactivate stop-migration signals that counteract the otherwise dominant promigratory action of ezrin in osteosarcoma cells.

*Oncogene* (2014) 33, 1912–1921; doi:10.1038/onc.2013.152; published online 6 May 2013

**Keywords:** CD99; osteosarcoma; cadherins; ezrin; ROCK2; ARP2/3

## INTRODUCTION

CD99 is a 32 kDa highly glycosylated transmembrane protein encoded by the *MIC2* gene.<sup>1</sup> Located in the pseudoautosomal region of sex chromosomes, *MIC2* encodes two distinct products by alternative splicing: a long form (32 kDa) corresponding to the full-length protein (CD99wt), and a short form harbouring a deletion in the cytoplasmic domain (CD99sh) (28 kDa).<sup>2</sup> CD99 is involved in multiple cellular events including cell adhesion, apoptosis, differentiation of T-cells and thymocytes, transendothelial migration of leukocytes, maintenance of cellular morphology and regulation of intracellular vesicular protein trafficking<sup>3–13</sup> both in physiology and in pathological conditions. Though its biological functions are quite well defined, the molecular mechanisms underlying CD99-mediated phenotypes are still controversial and clearly dependent on the cellular context. In fact, the expression of CD99 is high and associated with tumour progression in Ewing sarcoma and acute lymphoblastic leukaemia<sup>14,15</sup> while in osteosarcoma<sup>16,17</sup> and Hodgkin's lymphoma,<sup>18</sup> CD99 is expressed at low levels and functions as a tumour suppressor. In addition, the two alternative spliced isoforms are also reported to be expressed in a cell-type specific

manner and associated with distinct functional outcomes in relation to apoptosis, differentiation and migration/invasion.<sup>17,19–21</sup> CD99sh expression increases MMP9 activity and stimulates the migration and metastasis of breast cancer<sup>21</sup> and osteosarcoma,<sup>17</sup> whereas CD99wt significantly inhibits malignancy in osteosarcoma.<sup>16</sup> Thus, molecular dissection of the mechanisms associated with the differential cell migration capabilities induced by the two alternative CD99 isoforms may help to identify new treatment options for anticancer therapy targeting invasion and metastasis. In this study, we show that the expression of CD99wt induces recruitment of N-cadherin and  $\beta$ -catenin to cell membrane adherens junctions. Classical cadherins mediate cell–cell interactions through their extracellular domains, whereas their cytoplasmic tails bind to the members of the armadillo protein family, such as  $\alpha$ - and  $\beta$ -catenin to communicate with actin cytoskeleton.<sup>22</sup> In epithelial cells, E-cadherin is an invasion suppressor, whereas N-cadherin induces morphological changes toward a fibroblastic phenotype, rendering the cells more motile and invasive.<sup>23</sup> On the contrary, in osteosarcoma N-cadherin behaves as a tumour suppressor inhibiting cell migration and metastasis formation,<sup>24,25</sup> thus mirroring functions of CD99. In

<sup>1</sup>Department of Experimental, Diagnostic and Specialty Medicine, University of Bologna, Bologna, Italy; <sup>2</sup>CRS Development of Biomolecular Therapies, Bologna, Italy;

<sup>3</sup>Experimental Oncology Laboratory, Istituto Ortopedico Rizzoli, Bologna, Italy; <sup>4</sup>PROMETEO Laboratory, STB, RIT Department, Istituto Ortopedico Rizzoli, Bologna, Italy and

<sup>5</sup>Department of Biomedical and Neuromotor Sciences, University of Bologna, Bologna, Italy. Correspondence: Dr K Scotlandi, CRS Development of Biomolecular Therapies, Istituto Ortopedico Rizzoli, Via di Barbiano 1/10, 40136 Bologna, Italy.

E-mail: katie.scotlandi@ior.it

Received 16 July 2012; revised 25 February 2013; accepted 8 March 2013; published online 6 May 2013

addition, forced expression of CD99wt inhibits the expression of several molecules crucial to actin remodelling, such as actin-related protein 2 homologue (yeast) (*ACTR2*), Actin-related protein 2/3 complex, subunit 1A (*ARPC1A*) and Rho-associated, coiled-coil containing protein kinase 2 (*ROCK2*), as well as ezrin, an ezrin/radixin/moesin family member that has been clearly associated with tumour progression and metastatic spread of osteosarcoma.<sup>26,27</sup> Functional studies point to *ROCK2* as a crucial mediator of the CD99-induced mechano-transcriptional pathways regulating metastasis in osteosarcoma.

## RESULTS

CD99wt fortifies osteosarcoma cell–cell adhesion and favours recruitment of N-cadherin and  $\beta$ -catenin at the membrane level. Forced expression of CD99wt interfered with spontaneous cell aggregation and migration of osteosarcoma cells, by increasing their cell–cell adhesion, and dramatically decreasing their migratory ability.<sup>16,17</sup> Ultrastructural analysis indicates the formation of rudimentary adherens junctions in cells overexpressing CD99wt in comparison with the parental cell line (Figure 1a). Accordingly, we also observed increased expression of N-cadherin and  $\beta$ -catenin (Figures 1b and c), which were both well recruited at the cell membrane in contrast to what observed in the highly migrating CD99sh-expressing cells (Figure 1d). In keeping with the different migratory ability of parental and CD99wt or CD99sh cells, a differential pattern of actin organisation was observed (Figure 1b). As  $\beta$ -catenin also serves as a transcriptional activator in the canonical Wnt signalling pathway when not bound to cadherins, we checked Wnt-luciferase activity in our model. As previously reported,<sup>28</sup> the Wnt/ $\beta$ -catenin pathway appears to be barely active in osteosarcoma cells, regardless of the CD99 levels of expression (Figure 1e). Consistent with the low, if any,  $\beta$ -catenin nuclear activity in osteosarcoma, immunostaining did not detect the molecule in the nucleus either *in vitro* or in clinical samples (nuclear positivity: 0/77; Supplementary Figure 1). When expressed at high levels  $\beta$ -catenin was always detected on the plasma membrane, further supporting its role in cell adhesion (low expressors: 41/77, 53%; high expressors: 36/77, 47%).

### Identification of *ROCK2* as a crucial mediator of CD99-regulated osteosarcoma cell adhesion and migration

To determine the molecular basis of CD99 function in osteosarcoma, we analysed the gene expression profile of CD99wt-expressing cells compared with U-2OS parental cells. Annotation analysis with the GeneGo MetaCore platform identified a number of significantly modulated pathways. The top ten are shown in Supplementary Figure 2. The highest scoring pathway was 'cytoskeleton remodelling-TGF, WNT and cytoskeleton remodelling'. Among the genes belonging to this pathway (Supplementary Table 2), we focused on *ACTR2* (also named *ARP2*), *ARPC1A* and *ROCK2*, three genes that are downregulated in CD99wt cells and are reported to be functionally connected with actin cytoskeleton remodelling and with cell migration. Both *ARP2* and *ARPC1A* encode for two out of seven subunits of the human Arp2/3 complex, which is essential for cell motility through lamellipodial actin assembly and protrusion<sup>29</sup> while *ROCK2* encodes a serine/threonine kinase, which regulates the formation of actin stress fibres, focal adhesions and cellular myosin-based contractility.<sup>30</sup> Consistent with its functional role as an actin nucleator, *ARP2* showed a high and polarised expression in the cytoplasm of the highly migrating U-2OS and CD99sh cells (Figure 2a, arrows) but was barely present, if not at all, in the poorly migrating CD99wt transfectants. In keeping with the genetic data, western blot analysis and immunofluorescence also revealed downregulation of *ROCK2* in CD99wt transfectants, compared to parental U-2OS cell line and CD99sh-expressing cells (Figure 2a). Whenever *ROCK2*

function was inhibited by using *N*-(2-(2-(dimethylamino)ethoxy)-4-(1H-pyrazol-4-yl)phenyl)-2,3-dihydrobenzo[b]<sup>1,4</sup>dioxine-2-carboxamide (Stemolecule *ROCK2* Inhibitor) (Stemgent, San Diego, CA, USA), homotypic aggregation of U-2OS and U-2/CD99sh, but not of U-2/CD99wt cells was increased whereas cell motility was remarkably reduced (Figure 2b). Pharmacological inhibition of *ROCK2* also induced concomitant upregulation of  $\beta$ -catenin and N-cadherin in parental and CD99sh-expressing cells, whereas *ARP2* expression did not change (Figures 2c and d). This was confirmed in another experimental model. Saos-2 cells overexpressing CD99wt showed reversion of the malignant phenotype.<sup>16,17</sup> In keeping with their decreased migratory capabilities (Supplementary Figure 3), Sa/CD99wt cells showed reduced expression of *ARP2* and *ROCK2* (Figure 3a) together with increased expression and recruitment of  $\beta$ -catenin and N-cadherin at the cell membrane (Figure 3b).

To confirm the functional association between *ROCK2* and the expression of molecules involved in cell adhesion and cytoskeleton remodelling, we either transiently silenced the expression of *ROCK2* in Saos-2 and U-2OS cells by small interfering RNA (siRNA) sequences or induced re-expression of *ROCK2* in cells with CD99wt. Cells deprived of *ROCK2* (Supplementary Figure 4) showed increased homotypic aggregation as well as reduced cell migration, whereas the re-expression of *ROCK2* (Supplementary Figure 4) rescued the observed phenotypes (Figure 3c). Consistently, we found increased expression of  $\beta$ -catenin and N-cadherin on the cell surface of cells deprived of *ROCK2* (Figure 3d), further supporting the key role of *ROCK2* in regulating these mechano-transcription pathways. By contrast, no modulation was observed in *ARP2* staining, indicating that the expression of *ARP2*, though a mirror of the migratory phenotype of osteosarcoma cells, is not functionally connected with *ROCK2*.

### CD99wt suppresses ezrin and increase both $\beta$ -catenin and N-cadherin expression through modulation of Src and *ROCK2* activity

*ROCK2* was found to be involved in disruption of adherens junctions, increase of motility and formation of actin-rich structures containing ezrin.<sup>31</sup> As ezrin in osteosarcoma is linked to increased tumour migration and lung metastasis,<sup>26,32,33</sup> both dramatically inhibited by CD99wt, we analysed the expression of ezrin and its Thr567 phosphorylated form in relation to *ROCK2* in our experimental model. Consistently, with the suppression of metastatic capabilities of CD99wt overexpressing cells, the expression of ezrin, Thr567-p-ezrin and the ezrin/radixin/moesin protein family were found to be significantly decreased at protein level (Figures 4a and b) but not transcriptional level (Supplementary Figure 5) when compared with parental and CD99sh cells. Osteosarcoma primary tumours generally expressed ezrin (45/53, 85%), with 62% of patients (33/53) showing high levels of expression (Supplementary Figure 1). CD99 was found to be completely negative in 70% of cases (54/77). High expression of CD99 was only detected in 10% (8/77) of tissue samples, whereas 20% (16/77) showed weak positivity. An inverse correlation was observed between CD99 and ezrin expression in clinical samples ( $r = -0.31$ ,  $P = 0.02$ ), further indicating functional connections between the two molecules. The specific inhibition of *ROCK2* or its silencing decreased ezrin expression (Figures 4c and d). Dose-dependent inhibition of ezrin was observed after cell exposure to *ROCK2* inhibitor (Figure 4e).

CD99 did not immunoprecipitate with ezrin,  $\beta$ -catenin or N-cadherin (Supplementary Figure 6), indicating an indirect regulation mechanism. We have previously reported that CD99wt co-immunoprecipitates with caveolin-1 and Src, forming a complex that maintains Src in its inactive conformation.<sup>16,17</sup> As Src is also involved in regulation and phosphorylation of *ROCK2*,<sup>34,35</sup> we analysed the functional association between Src,

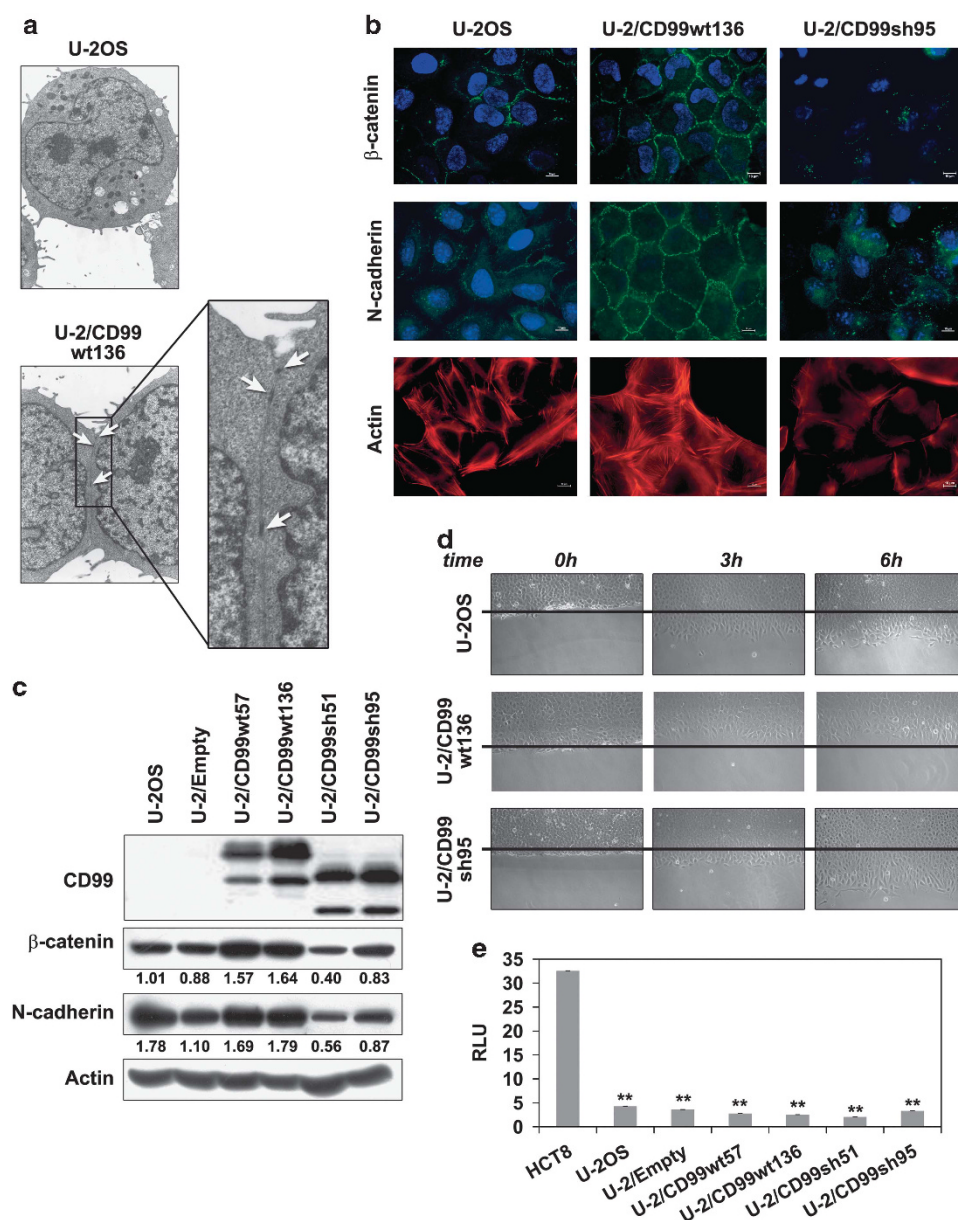


**Figure 1.** CD99 expression induces adherence junctions and recruitment of  $\beta$ -catenin and N-cadherin on the cell surface, while inhibiting migration of osteosarcoma cells. **(a)** Ultrastructural analysis of U-2/CD99wt136, which overexpresses the wild-type isoform of CD99 (CD99wt), as compared with the parental osteosarcoma cell line U-2OS. The inset shows the formation of cell junctions (arrows) in the CD99wt transfectant. TEM, magnification  $\times 22\,000$ . **(b)** Immunostaining of  $\beta$ -catenin and N-cadherin in U-2OS cell line compared with clones overexpressing the wild type (CD99wt) or truncated (CD99sh) isoforms of CD99. Actin filaments were detected by staining with PE-conjugated phalloidin. Digital images were taken in identical conditions using the image analysis software Nis Elements (Nikon Instruments s.p.a., Florence, Italy). Magnification  $\times 600$ , scale bar,  $10\,\mu\text{m}$ . **(c)** Western blotting of  $\beta$ -catenin and N-cadherin in U-2OS parental cell line and CD99-derived clones. Equal loading was monitored by anti-actin blotting. Densitometric analysis values for the  $\beta$ -catenin/actin and N-cadherin/actin ratios are expressed as adjusted volume optical density ( $\text{OD}/\text{mm}^2$ ). **(d)** Wound healing assay in U-2OS cells and CD99-derived clones. Pictures were taken at time 0, and after 3 or 6 h. Magnification  $\times 100$ . **(e)** Wnt-luciferase activity of U-2OS and CD99-derived clones. HCT-8, a colorectal adenocarcinoma cell line with a constitutively active Wnt pathway, was included as a positive control. For each sample the firefly/renilla luciferase ratio, normalised on the respective negative control, was shown as relative luciferase unit (RLU). Each column represents the mean  $\pm$  s.e. of at least two separate experiments performed in triplicate.  $^{**}P < 0.001$ , paired Student's *t*-test.

ROCK2, ezrin, N-cadherin and  $\beta$ -catenin in our experimental models. When cells were exposed to herbimycin, a Src inhibitor, we observed concomitant inhibition of ROCK2 and ezrin expression as well as simultaneous increase of  $\beta$ -catenin and N-cadherin levels (Figures 5a and b). To provide further evidence of a functional relationship between Src and ROCK2, we took advantage of the CD99 mutants.<sup>17</sup> Ser168, a residue of the cytoplasmic portion of the molecule missing from the truncated

short CD99 isoform, was found to be an important CD99 motif in the inhibition of migration and metastasis in U-2OS osteosarcoma cells. Lack of it, whether due to specific mutations (as in U-2/CD99mutS168 clones) or due to complete absence (as in CD99sh clones), resulted in disappearance of the negative impact of CD99wt on migration, whereas its presence in cells expressing CD99wt is sufficient to inhibit migration and metastasis. In contrast, cells expressing CD99 mutated at Tyr146 (U-2/



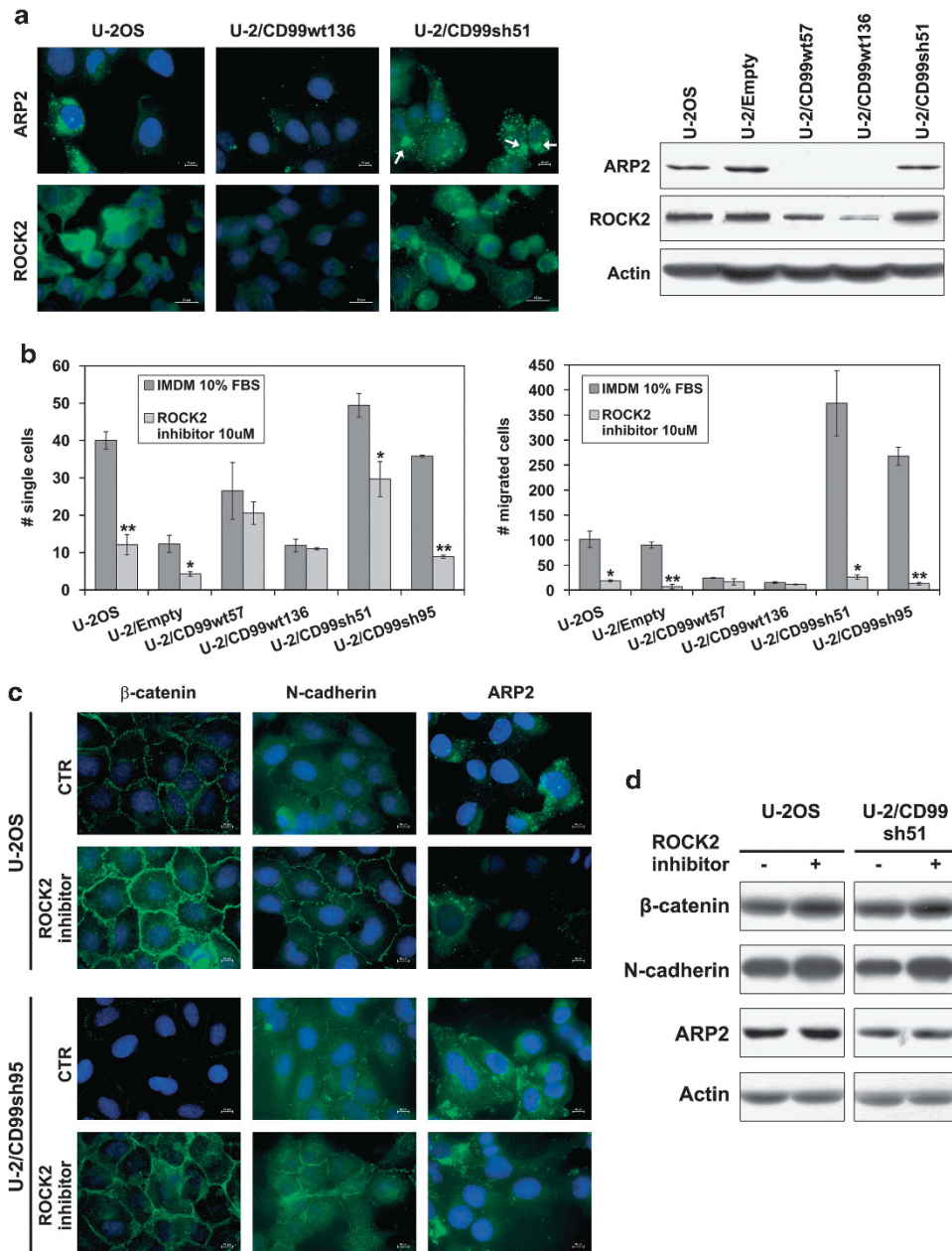


**Figure 2.** CD99-induced ROCK2 inhibition modifies adhesive and migratory properties of osteosarcoma cells. **(a)** Immunostaining and western blot expression of ARP2 and ROCK2 on CD99wt and CD99sh cells compared to the U-2OS parental cell line. Equal loading was monitored by anti-actin blotting. Digital images were taken in identical conditions using the image analysis software Nis Elements (Nikon Italia). Magnification  $\times 600$ , scale bar, 10  $\mu$ m. **(b)** Effect of the Stemolecule ROCK2 Inhibitor (10  $\mu$ M) on homotypic cell aggregation and migration of the U-2OS parental cell line and CD99-derived clones. Each column represents the mean  $\pm$  s.e. of at least two separate experiments performed in triplicate.  $*P < 0.05$ ;  $**P < 0.001$ , paired Student's *t*-test. **(c)** Immunostaining of  $\beta$ -catenin, N-cadherin and ARP2 expression in cells exposed to the Stemolecule ROCK2 Inhibitor (10  $\mu$ M) for 12 h. Digital images were taken in identical conditions using the image analysis software Nis Elements (Nikon Instruments s.p.a.). Magnification  $\times 600$ , scale bar, 10  $\mu$ m; **(d)** expression of  $\beta$ -catenin, N-cadherin and ARP2 in the U-2OS parental cell line and in U-2/CD99sh51 exposed to the Stemolecule ROCK2 Inhibitor (10  $\mu$ M) for 12 h by western blotting. Equal loading was monitored by anti-actin blotting.

CD99mutY146), a residue located in the intracellular residue common to the two isoforms, exhibited behaviour similar to those expressing the long CD99wt isoform. The level of c-Src phosphorylation was significantly reduced in U-2/CD99wt and U-2/CD99mutY146, but not in U-2/CD99sh and U-2/CD99mutS168, as compared to the parental cell line (ratio p-Src/Src: 0.342 in U-2OS;  $0.15 \pm 0.01$  in U-2/CD99wt,  $0.073 \pm 0.05$  in U-2/CD99mutY146,  $0.839 \pm 0.143$  in U-2/CD99sh,  $0.649 \pm 0.07$  in U-2/

CD99mutS168).<sup>17</sup> Accordingly, the expression of ROCK2, ezrin, Thr567-p-ezrin and ezrin/radixin/moesin were inhibited in U-2/CD99mutY146, somewhat as observed in U-2/CD99wt, but was reverted to the levels of the parental U-2OS cell line following mutation of the Ser168 residue (Figure 5c). These data confirm the existence of a ROCK2, ezrin, and migration/metastasis axis that may be reversed by CD99wt expression through modulation of Ser168 residue and c-Src activity.

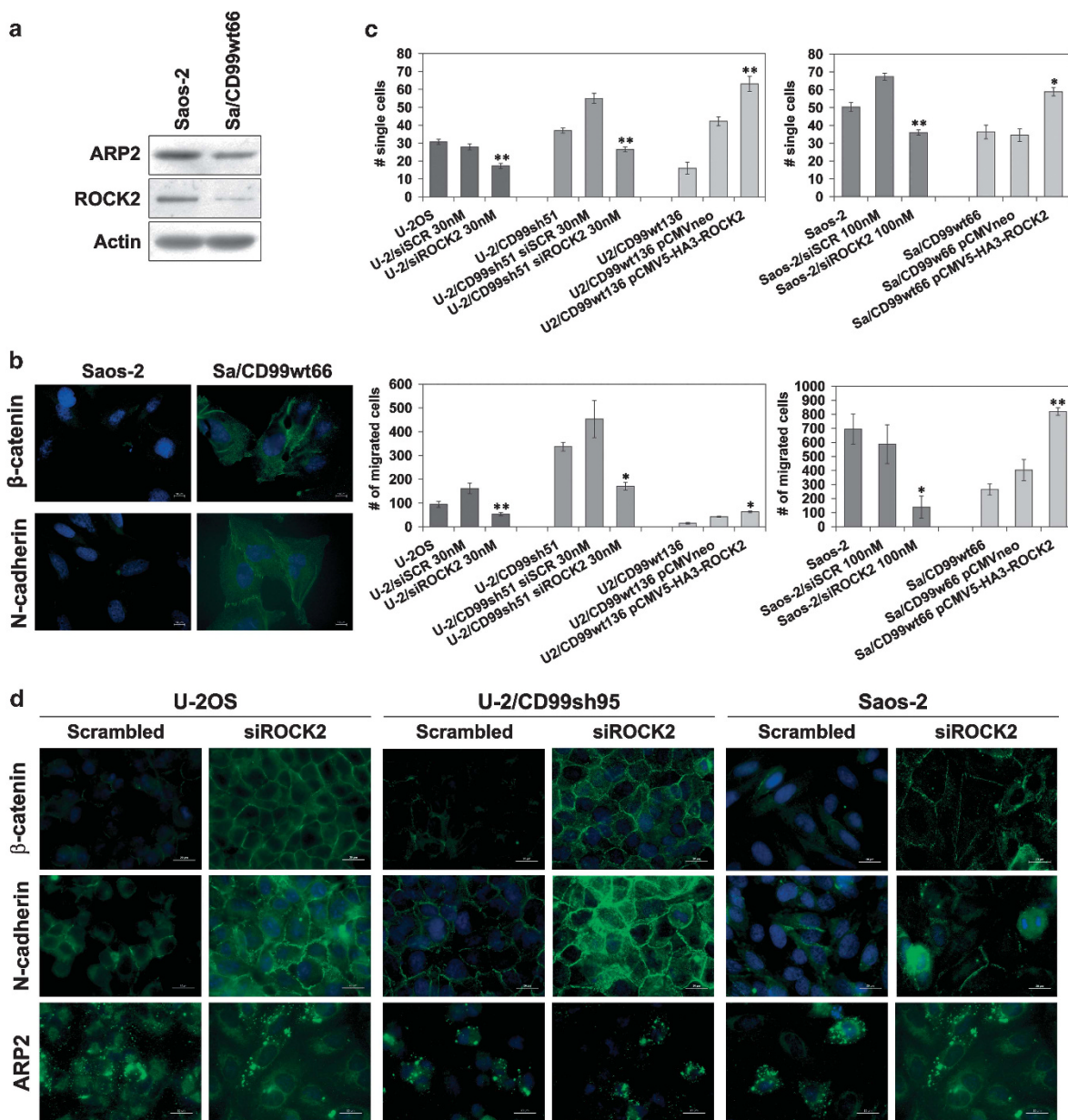


**Figure 3.** Silencing or overexpression of ROCK2 confirm the molecule as a functionally important mediator of OS cell migration and adhesion. **(a)** Western blotting of ARP2 and ROCK2 in Saos-2 and Sa/CD99wt66. Equal loading was monitored by anti-actin blotting. **(b)** Immunostaining of  $\beta$ -catenin and N-cadherin in Saos-2 and Sa/CD99wt66. Digital images were taken in identical conditions using the image analysis software Nis Elements (Nikon Italia). Magnification  $\times 600$ , scale bar,  $10\ \mu\text{m}$ . **(c)** ROCK2 silencing by siRNA sequences significantly increased homotypic aggregation while inhibiting migration of osteosarcoma cells. Opposite behaviour was shown when ROCK2 expression was rescued in CD99wt transfected cells. Each column represents the mean  $\pm$  s.e. of at least two separate experiments performed in triplicate. \* $P < 0.05$ ; \*\* $P < 0.001$ , paired Student's *t*-test. **(d)** Immunostaining of  $\beta$ -catenin, N-cadherin and ARP2 in cells silenced for ROCK2 expression. Digital images were taken in identical conditions using the image analysis software Nis Elements (Nikon Instruments s.p.a.). Magnification  $\times 600$ , scale bar,  $20\ \mu\text{m}$ .

## DISCUSSION

Regulation of cell adhesion and migration is an essential component of the metastatic process. Although cancer cells possess a broad spectrum of invasion and migration mechanisms, two main modes of tumour cell invasion into the surrounding tissues have been described: mesenchymal fibroblast-like migration, with elongated cells that have stress fibres and dependent on extracellular proteolysis, and amoeboid migration, which is characterised by round cells with high cortical tension and low adhesion to matrix.<sup>36</sup> Although these two modes of migration can be readily separated *in vitro*, the evidence suggests that they are

not mutually exclusive and that cells can convert from one type to another in response to changes in the microenvironment.<sup>37</sup> Cell-cell junctions are not maintained in either mesenchymal or amoeboid migration and actin cytoskeleton remodelling has a fundamental role in both processes. Indeed, the first step of cell migration commonly takes the form of dynamic filamentous actin cytoskeletal remodelling, which allows the formation of protrusions to adhere to the extracellular matrix in mesenchymal migration and generates intracellular contractile forces for cell movement in amoeboid migration.<sup>36</sup> These events are mediated by a complex and dynamic network of intracellular mediators, that



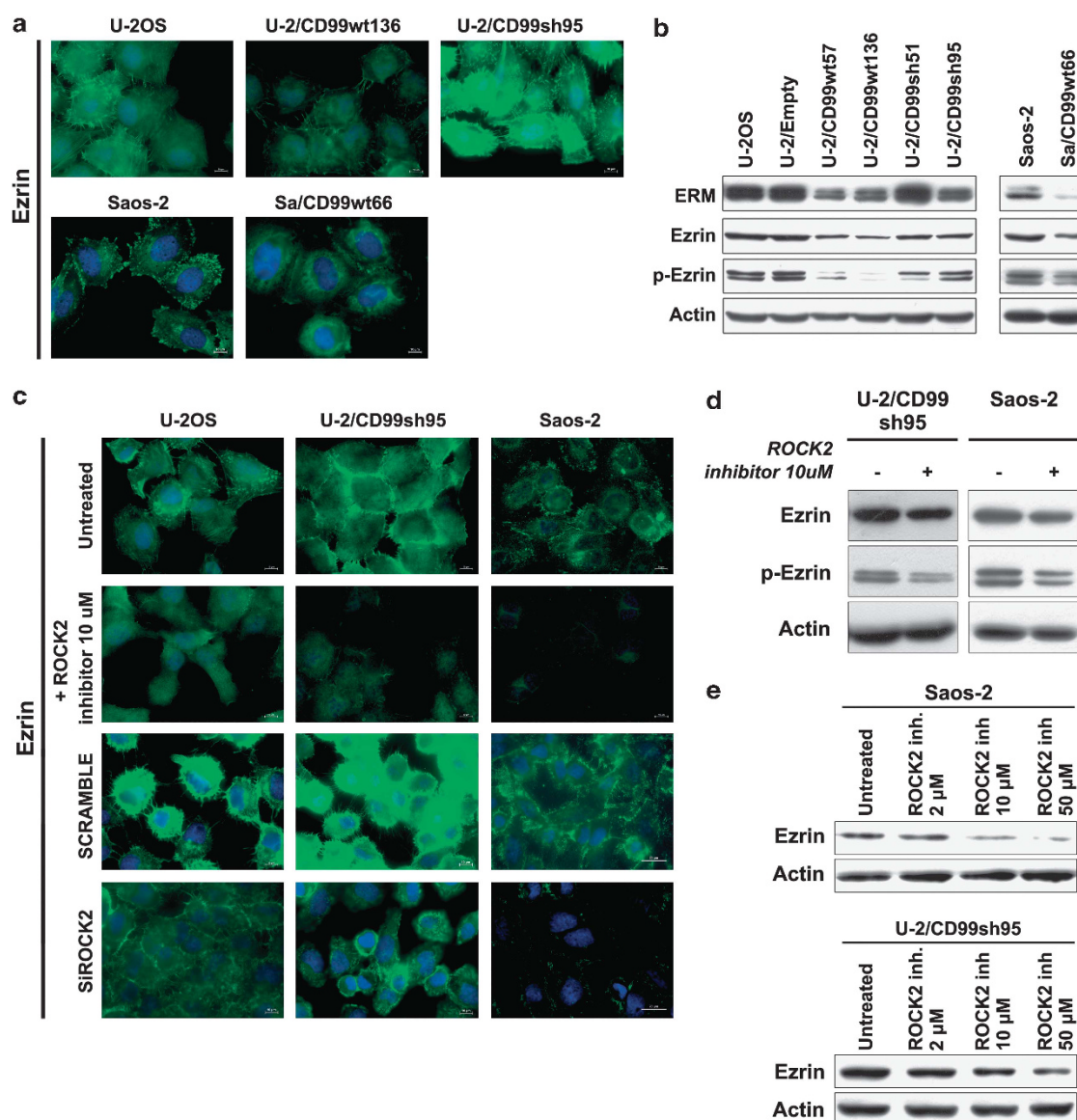


**Figure 4.** ROCK2 mediates the CD99-induced inhibition of ezrin in osteosarcoma cells. **(a)** Immunostaining of ezrin in U-2OS or Saos-2 parental cell lines and their CD99-derived clones. Magnification  $\times 600$ , scale bar, 10  $\mu\text{m}$ . **(b)** Western blotting expression of the ezrin-raxidin-moesin (ERM) family protein, ezrin and Thr567-p-Ezrin in U-2OS or Saos-2 parental cell lines and their CD99-derived clones. Equal loading was monitored by anti-actin blotting. **(c)** Fluorescent immunostaining of ezrin in cells treated with Stemolecule ROCK2 Inhibitor for 12 h or after ROCK2 silencing by siRNA sequences. Magnification  $\times 600$ , scale bar, 10  $\mu\text{m}$ . **(d)** Western blot analysis of ezrin and Thr567-p-Ezrin after 12 h exposure to the Stemolecule ROCK2 inhibitor. Equal loading was monitored by anti-actin blotting. **(e)** Dose-dependent ezrin inhibition by the Stemolecule ROCK2.

frequently work in a cell-specific manner. Interfering with elements that govern these mechanisms and control cell migration will diminish the opportunistic capacity of tumour cells to invade, migrate and metastasise at distal organs—a critical step in targeted intervention. In this paper, we have shown that forced expression of CD99wt in osteosarcoma cells induces downregulation of genes crucial for actin cytoskeleton remodeling and cell invasion, such as *ARP2*, *ARPC1A* (both belonging to the Arp2/3 complex) and *ROCK2*, together with increased adherens junction formation and recruitment of N-cadherin and  $\beta$ -catenin to the cell membrane.

Actin nucleation through the Arp2/3 complex is reported to be essential for tumour cell invasion in several experimental models.<sup>29</sup> Analysis of human cancers reveals strong expression of ARP2 in both stromal and tumour cells from colorectal

samples.<sup>38</sup> Moreover, silencing *ARPC1A* in pancreatic cancer cells leads to a dramatic decrease in cell invasion.<sup>39</sup> Accordingly, *ACTR2* and *ARPC1A* are downregulated when osteosarcoma cells acquire CD99wt expression, mirroring their decreased migratory capabilities. Because actin cytoskeleton dynamics constitute the driving force during cell migration, it is not surprising that ROCK2, a downstream effector of the Rho family of small monomeric GTPases, has been implicated in regulating CD99 effects on osteosarcoma cell migration. Rho proteins are known to have a pivotal role in tumour cell invasion and metastasis by regulating actin polymerisation at the leading edge of migrating cells, as well as the formation of stress fibres and focal adhesion assembly.<sup>40,41</sup> Both increase and decrease in the migration rate have been reported after ROCK inhibition, depending on the cell type.<sup>35,42–45</sup> However, although the two isoforms ROCK1 and 2 were generally

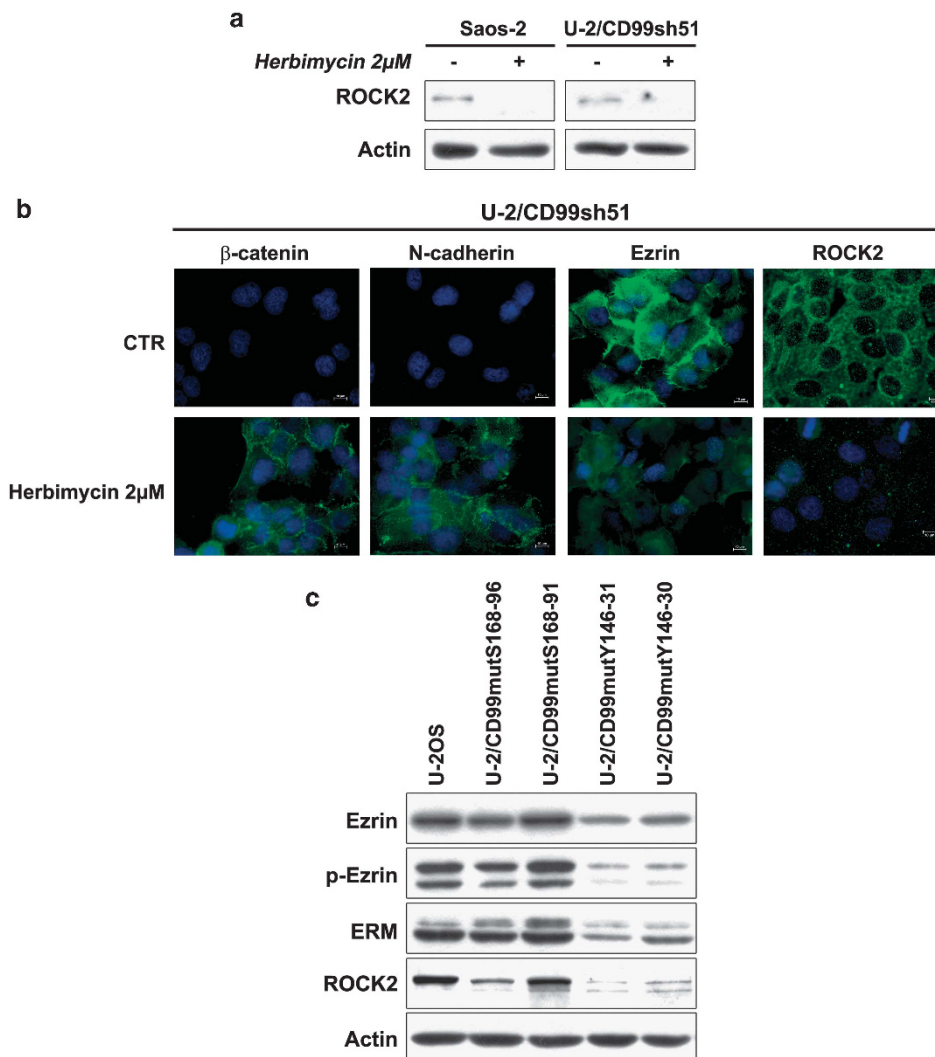


**Figure 5.** Inhibition of c-Src activity suppresses ezrin and ROCK2 while increasing N-cadherin and  $\beta$ -catenin. **(a)** Effect of herbimycin (2  $\mu$ M), a c-Src inhibitor, on ROCK2 expression in Saos-2 and U-2/CD99sh cells evaluated by western blotting. **(b)** Fluorescent immunostaining of  $\beta$ -catenin, N-cadherin, ezrin, and ROCK2, in U-2/CD99sh treated with herbimycin. Magnification  $\times 600$ , scale bar, 10  $\mu$ m. Digital images were taken in identical conditions using the image analysis software Nis Elements (Nikon Instruments s.p.a.); **(c)** Western blot expression of the ezrin/radixin/moesin (ERM) protein family, ezrin, Thr567-p-Ezrin, ROCK2 on U-2OS or CD99 mutants (U-2/CD99mutS168, U-2/CD99mutY146), which showed high or low Src activity, respectively.<sup>16</sup>

assumed to have the same functions, whenever a distinction between the two ROCKs has been drawn, ROCK2 depletion has been reported as enhancing microfilament bundle assembly into stress fibre and focal adhesion formation, whereas ROCK1 depleted cells show an opposite phenotype.<sup>46–48</sup> We observed a specific downregulation of ROCK2 in CD99wt-expressing cells, and modulation of it was functionally associated with modified adhesive and migratory behaviour by osteosarcoma cells. Cells inhibited for ROCK2 activity or cells deprived of ROCK2 expression display inhibited cell migration, as well as increased cell–cell adhesion and enhanced recruitment of adherens junction components like N-cadherin and  $\beta$ -catenin at the cell membrane. This is in line with other studies showing that ROCK2 activation results in disruption of adherens junctions, dissociation of cell clusters and increased motility.<sup>49</sup> In addition, high expression of ROCK2 has been associated with enhanced tumour invasion and progression in various types of tumours, including colon and bladder cancer,<sup>50,51</sup> testicular germ cell tumour<sup>52</sup> and hepatocellular carcinoma.<sup>53</sup>

Our previous data indicate that CD99 isoforms dictate opposite effects on cell migration and metastasis.<sup>17</sup> While CD99wt acts as a potent suppressor of these processes, cells expressing CD99sh regain or enhance their migration and metastatic ability. This opposite behaviour is associated with differential expression of ROCK2, and, interestingly enough, of ezrin too, a multifunctional protein that regulates cell adhesion and motility by connecting the actin cytoskeleton to the extracellular matrix.<sup>54</sup> Clinical data have indicated a positive association between ezrin expression and tumour progression in several tumours.<sup>55</sup> Ezrin is generally expressed at higher levels in sarcomas than in carcinomas and found to be necessary for osteosarcoma metastasis.<sup>26</sup> Small molecular inhibitors of ezrin have recently been proposed as a therapeutic approach to prevent osteosarcoma tumour metastasis.<sup>32</sup> Our present paper shows an inverse relationship between expression of CD99 and ezrin both in experimental and clinical samples. Osteosarcoma commonly does not express CD99 but expresses high levels of ezrin. By contrast, osteoblasts and osteocytes in the bone matrix generally strongly express CD99,<sup>16</sup>

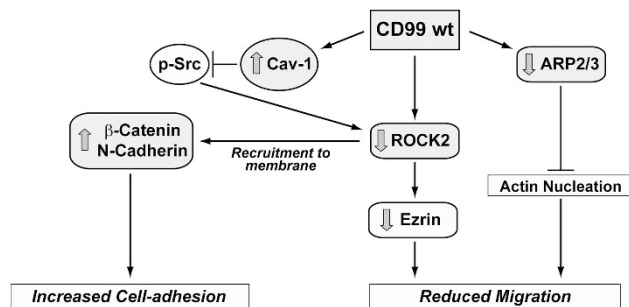


**Figure 6.** Schematic presentation of CD99wt effects on osteosarcoma cell adhesion and migration. CD99wt by inhibiting c-Src/ROCK2 axis leads to ezrin inhibition together with N-cadherin and  $\beta$ -catenin recruitment to the plasma membrane.

whereas poor immunoreactivity to the ezrin/radixin/moesin family proteins has been reported.<sup>56</sup> In our experimental models, when CD99wt expression was induced, the protein levels of ezrin decreased, and we demonstrated a functional connection with ROCK2. Phosphorylation of ezrin at Thr567 has been identified as a critical step in its conformational activation.<sup>57,58</sup> In its active form, ezrin functions as a crosslinker between the plasma membrane and the cortical cytoskeleton, favouring cellular movement. Although direct binding has been demonstrated for several adhesion-related proteins such as CD44 or CD95,<sup>59</sup> CD99 does not seem directly to associate with ezrin but rather controls ezrin indirectly through ROCK2. A c-Src/Akt/ROCK2 cascade has recently been shown to regulate ezrin status in fibroblast and tumour cells.<sup>31</sup> We reported increased or decreased c-Src kinase activity in cells alternatively expressing the two CD99 isoforms<sup>17</sup> and here, we show how inhibition of c-Src functions is associated with inhibition of ezrin and ROCK2 expression. We also demonstrate that the Ser168 residue of CD99 molecule has a pivotal role. Cells lacking Ser168 residue for specific mutations or deletion of larger intracytoplasmic fragment, are prevented from forming the CD99–caveolin-1–c-Src complex, which is required to maintain c-Src in its inactive conformation.<sup>17</sup> In keeping with the regaining of c-Src kinase activity, these cells restore ROCK2, ezrin and phospho-ezrin expression as well as migratory capabilities. Levels of phospho-ezrin were reduced or increased in parallel to levels of ezrin, indicating that ROCK2 affects ezrin by regulating its expression rather than its functions. Inhibition of c-Src and ROCK2 in overexpressing CD99wt cells also favours trafficking of N-cadherin and  $\beta$ -catenin at the plasma membrane, thus depicting a functional network that sustains cell adhesion and inhibits cell migration (Figure 6). We propose that the re-expression of CD99wt, a cell surface molecule, which is generally present in osteoblasts but lost in osteosarcoma, through inhibition of c-Src and ROCK2 activity, manages to induce a switch in the expression of the cell surface molecules that regulate actin cytoskeleton remodelling and cell movement. In particular, when the c-Src/ROCK2 axis is inhibited, ezrin decreases, or even disappears, while N-cadherin and  $\beta$ -catenin translocate to the plasma membrane and function as main molecular bridges for actin cytoskeleton. By favouring N-cadherin/ $\beta$ -catenin cell membrane recruitment, adherens junction formation and stable cell–cell interactions, the re-expression of CD99wt increases contact strength and reactivates stop-migration signals that counteract the otherwise dominant promigratory action of ezrin in osteosarcoma cells.

## MATERIALS AND METHODS

### Cell lines

Two parental osteosarcoma cell lines U-2OS and Saos-2 were obtained from the American Type Culture Collection (Manassas, VA, USA). Cells

overexpressing wild type (U-2/CD99wt57, U-2/CD99wt136, Sa/CD99wt66), truncated (U-2/CD99sh51 and U-2/CD99sh95), Ser168 mutated (U-2/CD99mutS168-91 and U-2/CD99mutS168-96) or Tyr146 mutated (U-2/CD99mutY146-30 and U-2/CD99mutY146-31) CD99 have been characterised previously.<sup>16,17</sup> Cells transfected with the empty vector pcDNA3 were used as negative control. Transfectants were maintained in IMDM containing 10% fetal bovine serum and 500  $\mu$ g/ml neomycin (Sigma, St Louis, MO, USA) to a maximum of eight *in vitro* passages. Cells were tested for mycoplasma contamination every 3 months (last check January 2013) by PCR mycoplasma detection set (Takara Bio Inc., Shiga, Japan) and authenticated by STR PCR analysis. DNA was extracted by each cell line with DNAzol (Invitrogen Life Technologies, Paisley, UK) and characterised by STR PCR analysis using genRESVR MPX-2 and genRESVR MPX-3 kits (Serac, Bad Homburg, Germany). The following loci were verified: D16S539, D18S51, D19S433, D21S11, D25S1338, D3S1358, D5S818, D8S1179, FGA, SE33, TH01, TPOX VWA (Institut für Rechtsmedizin, Forensische Molekularbiologie, Universitätsklinikum Düsseldorf, last control may 2012).

### Treatments

To inhibit ROCK2, cells were transfected with siRNA sequences directed against ROCK2 (ON-TARGETplus SMARTpool, Human ROCK2, Dharmacon, Chicago, IL, USA) or irrelevant targets (ON-TARGETplus Non-targeting siRNA) 24 h after cell seeding using the Lipofectamine 2000 transfection kit (Invitrogen Life Technologies). In addition, the ROCK2 inhibitor N-(2-(2-(dimethylamino)ethoxy)-4-(1H-pyrazol-4-yl)phenyl)-2,3-dihydrobenzo[b][1,4]dioxine-2-carboxamide (Stemolecule ROCK2 Inhibitor) as well as the c-Src inhibitor herbimycin (Calbiochem, San Diego, CA, USA) were used. Functional tests were performed after 24–72 h. To rescue ROCK2 expression in CD99wt cells, the expression vector pCMV5-HA3-ROCK2<sup>60</sup> was used.

### Ultrastructural analysis

Cells ( $5 \times 10^6$ ) were trypsinised, washed twice in phosphate-buffered saline and centrifuged. Cell pellets were fixed in glutaraldehyde 2.5% in cacodylate buffer 0.1 M, postfixed in osmium tetroxide 1%, dehydrated in ethanol and embedded in araldite. Thin sections, counterstained with uranyl acetate and lead citrate, were examined by a Philips 410 transmission electron microscope (Philips Research, Eindhoven, Netherlands).

### Motility and cell–cell adhesion assays

Cells ( $1 \times 10^5$ ) were treated with or without Stemolecule ROCK2 Inhibitor (10  $\mu$ M), with or without herbimycin (2  $\mu$ M) or with or without siRNA directed against ROCK2 (30–100 nM), after which they were analysed for migration and homotypic aggregation. The motility assay and the homotypic adhesion assay were performed as previously described.<sup>6,17</sup> The same set of experiments were done in CD99wt-expressing cells transiently transfected with the ROCK2 expression vector pCMV5-HA3-ROCK2 (20  $\mu$ g) to verify functional connexions.

### Immunofluorescence

Adherent cells grown on coverslips for 48 h were fixed in 4% paraformaldehyde and permeabilised with 0.15% Triton X-100 in phosphate-buffered saline or in methanol, and incubated with the following antibodies: anti-ARP2 (Santa Cruz Biotechnology, San Diego, CA, USA) (1:25), anti-N-cadherin (BD Transduction Labs, Lexington, KY, USA) (1:100), anti- $\beta$ -catenin (Santa Cruz Biotechnology) (1:50), anti-ezrin (Sigma) (1:200), anti-ROCK2 (Santa Cruz Biotechnology) (1:50). Goat anti-mouse FITC (Pierce Biotechnology, Rockford, IL, USA), (1:100), or polyclonal anti-rabbit FITC (Dako, Glostrup, Denmark) (1:80) were used as secondary antibodies. PE-conjugated phalloidin (5 U/ml) (Sigma) was applied for 30 min at room temperature to visualise actin filaments. Nuclei were counterstained with Hoechst 33256 (Sigma).

### Western blotting

Western blotting experiments were performed as previously described.<sup>16</sup> The following primary antibodies were employed: anti-ROCK2 (Santa Cruz Biotechnology) (1:1000); anti-ARP2 (Santa Cruz Biotechnology) (1:1000); anti-N-cadherin (BD Transduction Labs) (1:2500); anti- $\beta$ -catenin (Santa Cruz Biotechnology) (1:1000); anti-ezrin (Sigma) (1:5000); anti-ezrin-raxdydin-moesin (Chemicon International, Temecula, CA, USA) (1:1000); anti-phospho-ezrin (Y576) (Sigma) (1:2000); anti-CD99 (12E7, DAKO) (1:10 000). Anti-rabbit (GE Healthcare, Piscataway, NJ, USA), anti-mouse (GE Healthcare) or anti-goat (Santa Cruz Biotechnology) horseradish



peroxidase-linked secondary antibodies were employed and the signal was revealed by ECL western blotting detection reagents (EuroClone, Milan, Italy). To confirm equal loading, membranes were reblotted with anti-actin antibody (Chemicon International) (1:1 00 000). Densitometric analysis was performed using GS-800 Imaging Densitometer and Quantity One 4.6.9 software (Bio-Rad Laboratories, Hercules, CA, USA).

### Immunoprecipitation analysis

Total cell lysates were prepared with a buffer containing 10 mM Tris-HCl (pH 7.4), 150 mM NaCl, 1% Triton X-100, 5 mM EDTA, 1% Na-deoxycholate, 0.1% SDS and protease inhibitors. 500 µg of total cell lysates were incubated with 1.5 µg anti-CD99-12E7 MAb (kindly provided by G. Bernard, Unité INSERM 343, Hôpital de l'Archet, Nice, France). Protein G Plus/Protein A Agarose beads (Calbiochem) were used to immunoprecipitate proteins linked to the primary antibody. Western blotting analysis was then performed as described.

### Luciferase assay

Cells were seeded in triplicate in 24-well plates. After 24 h, cells were transfected with 0.4 µg/ml of the TCF/LEF reporter (β-catenin responsive promoter) together with positive or negative controls (Signal Reporter Assay Kit, Qiagen, Hilden, Germany) by Lipofectamine 2000 (Invitrogen Life Technologies). Luciferase assay (Dual Glo Luciferase Assay System, Promega, Madison, WI, USA) was performed 24 h after cell transfection according to the manufacturer's protocol, and luciferase activity was measured using GloMax Multi Detection System (Promega). The firefly/renilla luciferase ratio was calculated and each sample was then normalised on its respective negative control. HCT-8, a colorectal adenocarcinoma cell line with a constitutively active Wnt pathway, was used as a positive control.<sup>61</sup>

### Microarray analysis

Comparative hybridisations were performed on Human 1A (V2) Oligo Microarray slides (Agilent Technologies, Loveland, CO, USA) containing 18 716 oligo probes. Total RNA was extracted using the TRIzol extraction kit (Invitrogen Life Technologies) and employed to obtain labelled cRNA, according to the manufacturer's instructions (Low RNA Input Fluorescent Linear Amplification Kit, Agilent Technologies). cRNAs from two CD99wt overexpressing clones (U-2/CD99wt57; U-2/CD99wt136) were labelled with Cyanine 5-CTP (Cy5) (Perkin Elmer Life Sciences Inc., Boston, MA, USA), while the cRNA from U-2OS parental cell line was labelled with Cyanine 3 CTP (Cy3) and used as a common reference for all comparisons. U-2/CD99wt136 clone was chosen for biological duplicate.

Images were obtained using the GENEPIX 4000A scanner (Axon Instruments, Foster City, CA, USA) and GENEPIX PRO 3.0 software. Filtered data were imported into BRB-ArrayTools software and normalised by the LOWESS regression function. Genes with a significant differential expression were identified using significant analysis of microarrays. A false discovery rate of 3.8% was used as the threshold. For annotation analysis GeneGo MetaCore platform (Thomson Reuters, New York, NY, USA) was used. Microarray data are available at Gene Expression Omnibus database (<http://www.ncbi.nlm.nih.gov/geo/>) with the accession number GSE39072.

### Patients

Expression of CD99 and β-catenin was evaluated by immunohistochemistry in 77 primary osteosarcomas. For ezrin, only 53 tumours were analysed due to limited sample availability. All patients had been enrolled by the Rizzoli Institute between 1992 and 2009 and undergone surgery and neoadjuvant chemotherapy treatments based on the administration of doxorubicin, high-dose methotrexate, cisplatin and ifosphamide.<sup>62,63</sup> The study was approved by the Institutional Ethical Committee of the Rizzoli Institute. Clinicopathological features are shown in Supplementary Table 1.

### Quantitative real-time PCR

Quantitative RT-PCR was performed on CFX96 Real-Time PCR Detection System (Bio-Rad Laboratories) using SsoFast EvaGreen Supermix (Bio-Rad Laboratories). cDNA 5 ng was amplified with 300 or 400 nM specific primers. Primer sequences were as follows: Ezrin 5'-CGAAACCAATC AATGTCG-3'; 3'-CTATTCTTCCACAGACGGG-5'; GAPDH 5'-GGCCTCCAAGG AGTAAGACC-3'; 3'-ACTTAGAGGGGAGGAGTGC-5'; Tata Binding Protein (TBP) 5'-TGACAGGAGCAAGAGTGAA-3'; 3'-ACCACCCCTCGACACTAC AC-5' hydroxymethylbilane synthase (HMBS) 5'-CACGTGTCCTCCGGTACTCG CCG-3'; 3'-CACTAACGCACCCATGGG-5'. Samples were run in triplicate.

Amplification reactions were checked for non-specific products by dissociation curve analysis and agarose gel electrophoresis. Normalised gene expression values ( $\Delta\Delta C_{(t)}$ ) were calculated by CFX Manager software (Bio-Rad Laboratories) using the two reference genes showing the best stability across samples.

### Immunohistochemistry

An avidin-biotin-peroxidase procedure was used for immunostaining (Vector Laboratories, Burlingame, CA, USA). Sections were incubated with the following primary antibodies: anti-ezrin (Sigma) (1:1000), anti-β-catenin (Santa Cruz Biotechnology) (1:50), anti-CD99 013 (Signet, Dedham, MA, USA) (1:80), which recognises both CD99 isoforms. Samples were classified on the basis of the positivity score as follows: negative, when no staining was observed; 'low-expressors', when low positivity was present (for β-catenin, less than 25% of positive cells score 1; for CD99 or ezrin the staining intensity was scored as +/−, + − −); 'high-expressors', when widespread strong immunostaining (scored as + + −, + + +, + + + + in the great majority of the cells) was present.

### Statistical analysis

Differences among means were analysed using Student's *t*-test. Fisher's exact test was used for frequency data.

### CONFLICT OF INTEREST

The authors declare no conflict of interest.

### ACKNOWLEDGEMENTS

We are in debt to Cristina Ghinelli for editing the manuscript and to Anming Meng, Department of Biological Sciences and Biotechnology, Tsinghua University, Beijing 100084, China, for kindly providing the plasmid pCMV5-HA3-ROCK2. This work was supported by the Italian Association for Cancer Research (AIRC; IG10452 to K Scotlandi), the Liddy Shriver Sarcoma Initiative (international grant to K Scotlandi) and Ricerca Fondamentale Orientata (RFO 2010 to C Zucchini). Rosa Simona Pinca is a recipient of a fellowship from the Associazione Onlus 'il Pensatore: Matteo Amitrano' and 'Liberi di Vivere Luca Righi.'

### REFERENCES

- Levy R, Dillej J, Fox RI, Warnke R. A human thymus-leukemia antigen defined by hybridoma monoclonal antibodies. *Proc Natl Acad Sci USA* 1979; **76**: 6552–6556.
- Hahn JH, Kim MK, Choi EY, Kim SH, Sohn HW, Ham DI *et al*. CD99 (MIC2) regulates the LFA-1/ICAM-1-mediated adhesion of lymphocytes, and its gene encodes both positive and negative regulators of cellular adhesion. *J Immunol* 1997; **159**: 2250–2258.
- Bernard G, Breitmayer JP, de Matteis M, Trampont P, Hofman P, Senik A *et al*. Apoptosis of immature thymocytes mediated by E2/CD99. *J Immunol* 1997; **158**: 2543–2550.
- Bernard G, Raimondi V, Alberti I, Pourtein M, Widjenes J, Ticchioni M *et al*. CD99 (E2) upregulates alpha4beta1-dependent T-cell adhesion to inflamed vascular endothelium under flow conditions. *Eur J Immunol* 2000; **30**: 3061–3065.
- Bernard G, Zoccola D, Deckert M, Breitmayer JP, Aussel C, Bernard A. The E2 molecule (CD99) specifically triggers homotypic aggregation of CD4+ CD8+ thymocytes. *J Immunol* 1995; **154**: 26–32.
- Cerisano V, Aalto Y, Perdichizzi S, Bernard G, Manara MC, Benini S *et al*. Molecular mechanisms of CD99-induced caspase-independent cell death and cell-cell adhesion in Ewing's sarcoma cells: actin and zyxin as key intracellular mediators. *Oncogene* 2004; **23**: 5664–5674.
- Husak Z, Printz D, Schumich A, Potschger U, Dworzak MN. Death induction by CD99 ligation in TEL/AML1-positive acute lymphoblastic leukemia and normal B cell precursors. *J Leukoc Biol* 2010; **88**: 405–412.
- Imbert AM, Belaoui G, Bardin F, Tonnel C, Lopez M, Chabannon C. CD99 expressed on human mobilized peripheral blood CD34+ cells is involved in transendothelial migration. *Blood* 2006; **108**: 2578–2586.
- Jung KC, Kim NH, Park WS, Park SH, Bae Y. The CD99 signal enhances Fas-mediated apoptosis in the human leukemic cell line, Jurkat. *FEBS Lett* 2003; **554**: 478–484.
- Petersen RD, Bernard G, Olafsen MK, Pourtein M, Lie SO. CD99 signals caspase-independent T-cell death. *J Immunol* 2001; **166**: 4931–4942.
- Schenkel AR, Dufour EM, Chew TW, Sorg E, Muller WA. The murine CD99-related molecule CD99-like 2 (CD99L2) is an adhesion molecule involved in the inflammatory response. *Cell Commun Adhes* 2007; **14**: 227–237.
- Schenkel AR, Mamdouh Z, Chen X, Liebman RM, Muller WA. CD99 plays a major role in the migration of monocytes through endothelial junctions. *Nat Immunol* 2002; **3**: 143–150.

- 13 Sohn HW, Choi EY, Kim SH, Lee IS, Chung DH, Sung UA *et al*. Engagement of CD99 induces apoptosis through a calcineurin-independent pathway in Ewing's sarcoma cells. *Am J Pathol* 1998; **153**: 1937–1945.
- 14 Dworzak MN, Froschl G, Printz D, Zen LD, Gaipa G, Ratei R *et al*. CD99 expression in T-lineage ALL: implications for flow cytometric detection of minimal residual disease. *Leukemia* 2004; **18**: 703–708.
- 15 Dworzak MN, Fritsch G, Fleischner C, Printz D, Froschl G, Buchinger P *et al*. CD99 (MIC2) expression in paediatric B-lineage leukaemia/lymphoma reflects maturation-associated patterns of normal B-lymphopoiesis. *Br J Haematol* 1999; **105**: 690–695.
- 16 Manara MC, Bernard G, Lollini PL, Nanni P, Zuntini M, Landuzzi L *et al*. CD99 acts as an oncosuppressor in osteosarcoma. *Mol Biol Cell* 2006; **17**: 1910–1921.
- 17 Scotlandi K, Zuntini M, Manara MC, Scindria M, Rocchi A, Benini S *et al*. CD99 isoforms dictate opposite functions in tumour malignancy and metastases by activating or repressing c-Src kinase activity. *Oncogene* 2007; **26**: 6604–6618.
- 18 Kim SH, Shin YK, Lee IS, Bae YM, Sohn HW, Suh YH *et al*. Viral latent membrane protein 1 (LMP-1)-induced CD99 downregulation in B cells leads to the generation of cells with Hodgkin's and Reed-Sternberg phenotype. *Blood* 2000; **95**: 294–300.
- 19 Alberti I, Bernard G, Rouquette-Jazdanian AK, Pelassy C, Pourtein M, Aussel C *et al*. CD99 isoforms expression dictates T-cell functional outcomes. *FASEB J* 2002; **16**: 1946–1948.
- 20 Lee EJ, Lee HG, Park SH, Choi EY, Park SH. CD99 type II is a determining factor for the differentiation of primitive neuroectodermal cells. *Exp Mol Med* 2003; **35**: 438–447.
- 21 Byun HJ, Hong IK, Kim E, Jin YJ, Jeoung DI, Hahn JH *et al*. A splice variant of CD99 increases motility and MMP-9 expression of human breast cancer cells through the AKT-, ERK-, and JNK-dependent AP-1 activation signaling pathways. *J Biol Chem* 2006; **281**: 34833–34847.
- 22 D'Souza-Schorey C. Disassembling adherens junctions: breaking up is hard to do. *Trends Cell Biol* 2005; **15**: 19–26.
- 23 Derycke LD, Bracke ME. N-cadherin in the spotlight of cell–cell adhesion, differentiation, embryogenesis, invasion and signalling. *Int J Dev Biol* 2004; **48**: 463–476.
- 24 Kashima T, Kawaguchi J, Takeshita S, Kuroda M, Takanashi M, Horiuchi H *et al*. Anomalous cadherin expression in osteosarcoma. Possible relationships to metastasis and morphogenesis. *Am J Pathol* 1999; **155**: 1549–1555.
- 25 Kashima T, Nakamura K, Kawaguchi J, Takanashi M, Ishida T, Aburatani H *et al*. Overexpression of cadherins suppresses pulmonary metastasis of osteosarcoma *in vivo*. *Int J Cancer* 2003; **104**: 147–154.
- 26 Khanna C, Wan X, Bose S, Cassaday R, Olomu O, Mendoza A *et al*. The membrane-cytoskeleton linker ezrin is necessary for osteosarcoma metastasis. *Nat Med* 2004; **10**: 182–186.
- 27 Park HR, Jung WW, Bacchini P, Bertoni F, Kim YW, Park YK. Ezrin in osteosarcoma: comparison between conventional high-grade and central low-grade osteosarcoma. *Pathol Res Pract* 2006; **202**: 509–515.
- 28 Cai Y, Mohseny AB, Karperien M, Hogendoorn PC, Zhou G, Cleton-Jansen AM. Inactive Wnt/beta-catenin pathway in conventional high-grade osteosarcoma. *J Pathol* 2010; **220**: 24–33.
- 29 Nurnberg A, Kitzing T, Grosse R. Nucleating actin for invasion. *Nat Rev Cancer* 2011; **11**: 177–187.
- 30 Riento K, Ridley AJ. Rocks: multifunctional kinases in cell behaviour. *Nat Rev Mol Cell Biol* 2003; **4**: 446–456.
- 31 Zheng S, Huang J, Zhou K, Zhang C, Xiang Q, Tan Z *et al*. 17beta-estradiol enhances breast cancer cell motility and invasion via extra-nuclear activation of actin-binding protein ezrin. *PLoS One* 2011; **6**: e22439.
- 32 Bulut G, Hong SH, Chen K, Beauchamp EM, Rahim S, Kosturko GW *et al*. Small molecule inhibitors of ezrin inhibit the invasive phenotype of osteosarcoma cells. *Oncogene* 2012; **31**: 269–281.
- 33 Kim C, Shin E, Hong S, Chon HJ, Kim HR, Ahn JR *et al*. Clinical value of ezrin expression in primary osteosarcoma. *Cancer Res Treat* 2009; **41**: 138–144.
- 34 Jiao X, Katiyar S, Liu M, Mueller SC, Lisanti MP, Li A *et al*. Disruption of c-Jun reduces cellular migration and invasion through inhibition of c-Src and hyperactivation of ROCK II kinase. *Mol Biol Cell* 2008; **19**: 1378–1390.
- 35 Lee HH, Tien SC, Jou TS, Chang YC, Jhong JG, Chang ZF. Src-dependent phosphorylation of ROCK participates in regulation of focal adhesion dynamics. *J Cell Sci* 2010; **123**: 3368–3377.
- 36 Pankova K, Rosel D, Novotny M, Brabek J. The molecular mechanisms of transition between mesenchymal and amoeboid invasiveness in tumor cells. *Cell Mol Life Sci* 2010; **67**: 63–71.
- 37 Wolf K, Mazo I, Leung H, Engelke K, von Andrian UH, Deryugina EI *et al*. Compensation mechanism in tumor cell migration: mesenchymal-amoeboid transition after blocking of pericellular proteolysis. *J Cell Biol* 2003; **160**: 267–277.
- 38 Otsubo T, Iwaya K, Mukai Y, Mizokami Y, Serizawa H, Matsuoka T *et al*. Involvement of Arp2/3 complex in the process of colorectal carcinogenesis. *Mod Pathol* 2004; **17**: 461–467.
- 39 Laurila E, Savinainen K, Kuuselo R, Karhu R, Kallioniemi A. Characterization of the 7q21-q22 amplicon identifies ARPC1A, a subunit of the Arp2/3 complex, as a regulator of cell migration and invasion in pancreatic cancer. *Genes Chromosomes Cancer* 2009; **48**: 330–339.
- 40 Hall A, Nobes CD. Rho GTPases: molecular switches that control the organization and dynamics of the actin cytoskeleton. *Philos Trans R Soc Lond, Biol Sci* 2000; **355**: 965–970.
- 41 Ridley AJ, Schwartz MA, Burridge K, Firtel RA, Ginsberg MH, Borisy G *et al*. Cell migration: integrating signals from front to back. *Science* 2003; **302**: 1704–1709.
- 42 Jaganathan BG, Ruester B, Dressel L, Stein S, Grez M, Seifried E *et al*. Rho inhibition induces migration of mesenchymal stromal cells. *Stem Cells* 2007; **25**: 1966–1974.
- 43 Borensztajn K, Peppelenbosch MP, Spek CA. Coagulation Factor Xa inhibits cancer cell migration via LIMK1-mediated cofilin inactivation. *Thromb Res* 2010; **125**: e323–e328.
- 44 Salhia B, Rutten F, Nakada M, Beaudry C, Berens M, Kwan A *et al*. Inhibition of Rho-kinase affects astrocytoma morphology, motility, and invasion through activation of Rac1. *Cancer Res* 2005; **65**: 8792–8800.
- 45 Zhang X, Li C, Gao H, Nabeka H, Shimokawa T, Wakisaka H *et al*. Rho kinase inhibitors stimulate the migration of human cultured osteoblastic cells by regulating actomyosin activity. *Cell Mol Biol Lett* 2011; **16**: 279–295.
- 46 Yoneda A, Mulhaupt HA, Couchman JR. The Rho kinases I and II regulate different aspects of myosin II activity. *J Cell Biol* 2005; **170**: 443–453.
- 47 Lock FE, Ryan KR, Poulter NS, Parsons M, Hotchin NA. Differential regulation of adhesion complex turnover by ROCK1 and ROCK2. *PLoS One* 2012; **7**: e31423.
- 48 Yoneda A, Ushakov D, Mulhaupt HA, Couchman JR. Fibronectin matrix assembly requires distinct contributions from Rho kinases I and -II. *Mol Biol Cell* 2007; **18**: 66–75.
- 49 Croft DR, Sahai E, Mavria G, Li S, Tsai J, Lee WM *et al*. Conditional ROCK activation *in vivo* induces tumor cell dissemination and angiogenesis. *Cancer Res* 2004; **64**: 8994–9001.
- 50 Kamai T, Tsujii T, Arai K, Takagi K, Asami H, Ito Y *et al*. Significant association of Rho/ROCK pathway with invasion and metastasis of bladder cancer. *Clin Cancer Res* 2003; **9**: 2632–2641.
- 51 Vishnubhotla R, Sun S, Huq J, Bulic M, Ramesh A, Guzman G *et al*. ROCK-II mediates colon cancer invasion via regulation of MMP-2 and MMP-13 at the site of invadopodia as revealed by multiphoton imaging. *Lab Invest* 2007; **87**: 1149–1158.
- 52 Kamai T, Yamanishi T, Shirataki H, Takagi K, Asami H, Ito Y *et al*. Overexpression of RhoA, Rac1, and Cdc42 GTPases is associated with progression in testicular cancer. *Clin Cancer Res* 2004; **10**: 4799–4805.
- 53 Wong CC, Wong CM, Tung EK, Man K, Ng IO. Rho-kinase 2 is frequently overexpressed in hepatocellular carcinoma and involved in tumor invasion. *Hepatology* 2009; **49**: 1583–1594.
- 54 Yu H, Zhang Y, Ye L, Jiang WG. The FERM family proteins in cancer invasion and metastasis. *Front Biosci* 2011; **16**: 1536–1550.
- 55 Bruce B, Khanna G, Ren L, Landberg G, Jirstrom K, Powell C *et al*. Expression of the cytoskeleton linker protein ezrin in human cancers. *Clin Exp Metastasis* 2007; **24**: 69–78.
- 56 Nakamura H, Ozawa H. Immunolocalization of CD44 and the ERM family in bone cells of mouse tibiae. *J Bone Miner Res* 1996; **11**: 1715–1722.
- 57 Fievet BT, Gautreau A, Roy C, Del Maestro L, Mangeat P, Louvard D *et al*. Phosphoinositide binding and phosphorylation act sequentially in the activation mechanism of ezrin. *J Cell Biol* 2004; **164**: 653–659.
- 58 Hamada K, Shimizu T, Matsui T, Tsukita S, Hakoshima T. Structural basis of the membrane-targeting and unmasking mechanisms of the radixin FERM domain. *EMBO J* 2000; **19**: 4449–4462.
- 59 Louvet-Vallee S. ERM proteins: from cellular architecture to cell signaling. *Biol cell* 2000; **92**: 305–316.
- 60 Zhang Y, Li X, Qi J, Wang J, Liu X, Zhang H *et al*. Rock2 controls TGFbeta signaling and inhibits mesoderm induction in zebrafish embryos. *J Cell Sci* 2009; **122**: 2197–2207.
- 61 Rivat C, De Wever O, Bruyneel E, Mareel M, Gerspach C, Attoub S. Disruption of STAT3 signaling leads to tumor cell invasion through alterations of homotypic cell-cell adhesion complexes. *Oncogene* 2004; **23**: 3317–3327.
- 62 Longhi A, Errani C, De Paolis M, Mercuri M, Bacci G. Primary bone osteosarcoma in the pediatric age: state of the art. *Cancer Treat Rev* 2006; **32**: 423–436.
- 63 Bacci G, Longhi A, Versari M, Mercuri M, Briccoli A, Picci P. Prognostic factors for osteosarcoma of the extremity treated with neoadjuvant chemotherapy: 15-year experience in 789 patients treated at a single institution. *Cancer* 2006; **106**: 1154–1161.

Supplementary Information accompanies this paper on the Oncogene website (<http://www.nature.com/onc>)